Negative DNA supercoiling tunes protein-mediated looping

Yan Yan[1,2,5], Wenxuan Xu[1,5], Sandip Kumar[1,3], Alexander Zhang[1], Fenfei Leng[4], David Dunlap[1], Laura Finzi[1*]

[1]Physics Department, Emory University, Atlanta, GA 30322 USA

[2]Current address: Wyss Institute for Biologically Inspired Engineering, Harvard University, Boston, MA 02115 USA

[3]Current address: Department of Biochemistry, University of Oxford, Oxford, OX1 3QU United Kingdom

[4]Department of Chemistry and Biochemistry, Florida International University, Miami, FL 33199 USA

[5]Co-first authors

Summary

Protein-mediated DNA looping is fundamental to gene regulation. Such loops occur stochastically in purified systems, but additional proteins and/or DNA supercoiling might tune looping for definitive responses. In lac repressor-mediated looping, the probabilities of loops in individual molecules ranged 0-100, and individual molecules exhibited representative behavior only in observations lasting an hour or more. Titrating with HU protein progressively compacted the DNA and increased the average probability of looping without narrowing the 0-100 distribution. Increased negative supercoiling also raised the average looping probability for the ensemble of molecules as well, but individual molecules more closely resembled the average. Furthermore, in only twelve minutes of observation, well within the shortest doubling time of the bacterium, most molecules exhibited the looping probability of the ensemble. DNA supercoiling, an inherent feature of all genomes, appears to be a fundamental determinant of time-constrained, emergent behavior in otherwise random molecular activity.

Keywords

Supercoiling; magnetic tweezer; HU protein; DNA looping; lac repressor; ergodicity; tethered particle motion

Introduction

Protein-mediated DNA looping is a ubiquitous regulatory process that compacts the genome and may regulate transcription, make DNA more, or less, accessible for replication, and facilitate repair (Brennan et al., 2017; Duderstadt et al., 2016; Hnisz et al., 2016; Priest et al., 2014a; Qian et al., 2016). Yet, in the thermal bath of the eukaryotic nucleus, or prokaryotic nucleoid, molecular motion is random and the behavior of a molecule can only be described in probabilistic terms (Nelson, 2003; Phillips R. et al., 2013). Single-molecule experimentation allows fluctuation

* Further information and requests for resources and reagents should be directed to and will be fulfilled by the Lead Contact and Corresponding author, Laura Finzi (lfinzi@emory.edu).

analysis (Bido et al.; Kundu et al., 2020; Milenkovic et al., 2020) and has revealed the robustly heterogeneous looping behavior of molecules (Datta and Seed, 2018; Finzi and Gelles, 1995; Graham et al., 2017; Kumar et al., 2016; Manzo et al., 2011; Manzo et al., 2012; Miyashita et al., 2015; Neuman et al., 2003; Wang et al., 1998; Zurla, 2009). Indeed, protein-mediated loops form and rupture stochastically in purified systems, and the lifetimes of such loops span several orders of magnitude. Thus, it is puzzling how a certain regulatory outcome can be achieved if it is based on random molecular interactions with broadly distributed probabilities.

Of course, the activity of biological molecules depends on their environment (Benkovic and Hammes-Schiffer, 2003) and there is evidence for sub-diffusive behavior of biomolecules in cells (Lubelski et al., 2008; Magdziarz et al., 2009; Meroz et al., 2010; Szymanski and Weiss, 2009). In addition, bacteria such as *E. coli* must contend with large variations in salt concentrations(Record et al., 1998). This suggests the existence of factors that tune looping dynamics and make probability homogeneous under a wide range of conditions (Cayley et al., 1991). Indeed, it was recently suggested that "hidden" variables tune random behavior (Golding, 2018) to produce a definitive outcome. One possibility might be nucleoid-associated proteins which are abundant in bacteria and are thought to decorate the bacterial genome, organizing and compacting the DNA(Lal et al., 2016; Macvanin and Adhya, 2012). Indeed, the HU protein seems a likely candidate, since knockouts and mutants profoundly modify the *E. coli* (K12) transcriptome(Hammel et al., 2016; Koli et al., 2011).

However, in an ergodic process, the range of individual behaviors in an ensemble can be observed in a single individual as well if observed for long enough (Moore, 2015; Palmer, 1982). Take for example, the titration curve of the probability of DNA looping versus the concentration of the lac repressor protein (LacI) that has been measured *in vivo* and *in vitro* (Priest et al., 2014a). The average looping probability was higher *in vivo* suggesting that accessory factors (proteins) or DNA topology enhanced the *in vivo* looping probability. Evidence that supercoiling might be important had already appeared in earlier reports of comparisons of LacI dissociation from linearized or supercoiled plasmids containing O1 and O2 separated by 400 base pairs (Whitson et al., 1987). Notably, different DNA molecules in the single molecule measurements behaved very differently during observations over a time span of approximately 30 min, comparable to the doubling time of *Escherichia coli* (*E. coli*) (Gibson et al., 2018), the bacterium in which LacI-mediated DNA looping is physiologically relevant. This suggested such hidden tuning parameters might be those that produce behavior representative of the ensemble in each member observed for a biologically relevant period.

In the experiments described below, the probability of DNA looping was measured versus various concentrations of the HU protein and levels of negative supercoiling. Only supercoiling significantly altered stochastic DNA looping by the Lac repressor to produce homogeneous behavior among a large set of molecules on the time scale of the bacterium.

Results

Previous work has shown that the probability of LacI-mediated looping in DNA molecules with two LacI binding sites (operators) depends on the protein concentration (Yan et al., 2018b). When LacI concentration is low, neither operator may be occupied by a LacI tetramer, the looping

probability is low, so the DNA tether remains extended, and the attached bead exhibits large excursions. When the concentration is too high, both operators become occupied by tetramers which, not being able to bind to each other, cannot form loops. Excursions are large for beads attached to these tethers as well. Only at intermediate concentrations, in which one tetramer may bridge two operators, does the probability of looping increase significantly. When loops form, the tether is less extended, and the excursions of the attached bead are restricted. Average looping probability is indicated by crosses in Figure 1, which summarizes ~30 min-long tethered particle motion (TPM) (Finzi and Gelles, 1995; Kovari et al., 2018; Kumar et al., 2014) measurements of LacI-mediated DNA looping between the strong O1 and weaker O2 operators separated by 400 bp (Yan et al., 2018b).

Although the average behavior of the population of DNA tethers is clear and follows expectation, the looping probabilities of individual DNA tethers under any given LacI concentration are very heterogeneous. Indeed, the whiskers of each box in the left panel of Figure 1, range from 0 to 100% looping probability. Raw data displaying this behavior is shown in representative temporal records for DNA tethers exposed to 0.5 nM LacI (Figure 1, right panel). Each time record corresponds to a different DNA tether. Unlooped states are depicted in red, and looped states are shown in blue and green corresponding to loops in anti-parallel or parallel configurations (Han et al., 2009a). Clearly, loop formation and breakdown occur randomly. However, some tethers are never looped, some are always looped, and some toggle between looped and unlooped states with various degrees of probability, calculated as the time spent in the looped state over the total observation time.

To verify that the heterogeneity observed was indeed due to the activity of single lac repressors and not variations among DNA molecules introduced during PCR, a control experiment was performed in which excursions of the tethered beads were monitored for 30 min, and then the first solution containing LacI was washed away with λ buffer supplemented with high salt concentration (1 M KCl). To verify washing, the excursions of the same tethered beads were then monitored for 20 min in which no looping was observed. Finally, an identical solution of protein was introduced into the microchamber and excursions of the bead were monitored for another 30 min. For comparison, the percentages of time spent by individual tethers in the looped state during the two observation periods (before and after washout of LacI) were calculated. Supplemental Figure S6 shows the lack of correlation between the looping probabilities measured on individual DNA tethers before and after, suggesting that the looping behavior of a DNA tether is dictated by variations in the activity of associated individual LacI proteins in the two observation periods. While there may be variation in the activity of individual LacI enzymes, the following experiments on supercoiled DNA molecules established conditions in which all DNA tethers exhibited a narrow range of looping probabilities within observations on the timescale of the doubling time of *E. coli*. Thus, activity variations do not appear to be significant.

Such extreme variation in the stability of lac-mediated loops might occur *in vivo*, but it is difficult to rationalize how it could benefit *E. coli* bacteria that should calibrate a response to lactose. Thus, there might be factors *in vivo* that tune the percentage of looping. Since protein-mediated looping is a ubiquitous regulatory mechanism across kingdoms, this question transcends the specific

organism and is relevant for cells of all organisms. We hypothesized that genome-compacting proteins and DNA supercoiling, which are common to all species, might decrease the variation in looping probability, because they compact DNA and reduce the distance between sites joined by the looping protein. As a model genome-compacting protein, we chose the nucleoid-associated protein HU which is abundant in bacteria, binds non-specifically to DNA, contributes to the overall architecture of the genome, and influences DNA replication and transcription (Bahloul et al., 2001; Berger et al., 2016; Morales et al., 2002; Rouvière-Yaniv et al., 1979; Yan et al., 2018a; Yan et al., 2018b).

To determine whether HU can eliminate variation in looping probabilities, tethered particle motion (TPM) experiments were conducted at one LacI concentration (2.5 nM) while the HU concentration was titrated from 0 to ~1 μM. The LacI concentration was chosen such that it would be easy to measure with negligible uncertainty, and increases or decreases in the looping probability would be obvious (Yan et al., 2018b). As shown previously by our lab and others, in the salt condition we use here, the magnitude of excursions of beads tethered to single DNA molecules decreases as HU concentrations increase (Xiao et al., 2010; Yan et al., 2018b); this protein-induced DNA compaction facilitates looping (Yan et al., 2018b). Indeed, as shown in the left panel of Figure 2, increasing the HU concentration increases the median looping probability driving it from around 20 to 80%. However, the looping probabilities of single DNA tethers ranged from 0 to 100% at each HU concentration as shown by the whiskers in the plot. The representative temporal traces in the right panel of Figure 2, show tethers that never looped, tethers that remained looped throughout the observation, and others that toggled between the looped and unlooped states. This is similar to what was observed for LacI-induced looping without additional factors (Figure 1), indicating that HU, despite its ability to compact DNA and favor looping overall, did not reduce the variation in the looping probabilities of different DNA tethers.

DNA supercoiling is a second factor responsible for genome compaction in live cells. It refers to the over- or under-winding of a DNA molecule, which is often quantified as the ratio of the number of turns added to a DNA molecule over the number of helical turns in the torsionally relaxed state. In live cells, DNA supercoiling is ubiquitous and dynamic, genomes are, in average, negatively supercoiled, and it has been shown that DNA unwinding under low, physiological forces compacts DNA in a way that facilitates looping by proteins (Yan et al., 2018b). Magnetic tweezers were used to modulate supercoiling and measure its effect on LacI-induced looping, focusing on the level of heterogeneity of the looping probabilities of different tethers. Magnetic tweezers are a convenient tool with which to modulate DNA supercoiling for *in vitro* experiments. Such tweezers utilize a magnet placed close to a microchamber with DNA tethering super-paramagnetic beads to the glass surface. The field attracts and orients the beads applying tension to the DNA. In addition, if the magnets are rotated, DNA will be twisted. If DNA is twisted under low tension, either winding or unwinding will induce plectonemes that decrease the extension of the DNA (Supplemental Figure S4).

Figure 3 summarizes measurements of LacI-mediated looping probability for the 2115 and 2011 bp DNA tethers unwound by different amounts under 0.45 pN of tension. Negative supercoiling progressively increased the looping probability (Yan et al., 2018b). The left panel in this figure

shows that increased (negative) supercoiling drove the looping probability from 0 to 100%. Note also that the looping probabilities measured for different DNA tethers are tightly grouped around the median values. Negative supercoiling dramatically reduced variation and produced a uniform, deterministic behavior. Similar behaviors were also observed with tensions of 0.25 and 0.75 pN (Supplemental Figure S7). This uniformity is illustrated in the right panel of Figure 3, where individual time traces, recorded under 0.45 pN of tension and -2.5 % supercoiling level, are quite similar and exhibit frequent switching between unlooped (red) and looped (blue/green) states.

Discussion

Supercoiling makes protein-mediated looping deterministic.

In the absence of supercoiling, the probabilities of LacI-mediated DNA looping for individual DNA tethers with, as well as without, HU range from 0 to 100%. In these conditions, in order for the protein to connect them, the LacI binding sites must juxtapose by 3-D diffusion opposed by a high energy barrier. HU protein helps to overcome this barrier and enhance looping by compacting the DNA to reduce the separation between the operators to be bridged. In contrast, supercoiling induces plectonemes which allow slithering of DNA segments past one another (Kim et al., 2018; van Loenhout et al., 2012). Thus, the operators may juxtapose through 1-D diffusion, across a much lower energy barrier. Negligible bending energy changes accompany slithering and little configurational entropy is lost when LacI connects two sites in a plectoneme. By reducing the dimensionality of the path to juxtaposition, supercoiling produced homogeneous looping probabilities for different DNA tethers that could not be achieved by adding HU to facilitate juxtaposition in three dimensions.

Since HU binding is known to supercoil DNA (Guo and Adhya, 2007), it might similarly alter looping in a torsionally constrained DNA tether. This was not possible in a TPM experiment (Figure 2) in which single-bond attachments of the DNA to the surfaces would swivel to release any torsion. However, previously published data (Yan et al., 2018b) showed that 1056 mM HU which produces a median value of 85% looping in DNA tethers under no tension (Fig. 2), produced just 30 or 15% average looping probabilities in DNA tethers under 0.25 or 0.45 pN of tension, respectively. This suggests that HU binding negligibly supercoils DNA in the conditions used here. To verify this, extension versus twist curves were measured for DNA in the presence of HU. In this assay, any unwinding associated with protein or small molecule binding to the DNA will alter the intrinsic twist of the molecule and shift the maximum extension of the molecule with respect to that of bare DNA (Lipfert et al., 2010; Salerno et al., 2010; Vlijm et al., 2017). As can be seen in Supplemental Figure S8, increasing the concentration of HU up to 1000 nM steadily contracted a DNA tether stretched by 0.45 pN in 200 mM KCl but negatively supercoiled the molecule by only -1.35 turns. This is equivalent to 0.4% supercoiling, which is insufficient to produce writhe (Brutzer et al., 2010). Thus, HU enhances looping by contracting DNA tethers but does not change the dimensionality of looping to promote uniform looping dynamics.

Figure 4 is an illustration of hypothetical energy landscapes for looping, which involves bending and possibly twisting the DNA molecule, as shown in the cartoons on the left. Energy is color-encoded according to the scale at right. The end-to-end distance of the loop segment is represented along the vertical axis. Near-zero end-to-end distance corresponds to the looped state, while the

unlooped states are more extended, up to 400 bp. The horizontal axis indicates the supercoiling in the DNA and its handedness. Panel (*A*) describes the experimental conditions in a TPM measurement, with no applied tension or torsion. The DNA may coil, bend, and juxtapose the two operators via 3-D diffusion, as shown in the superimposed cartoon. Different pathways may be followed through the broad and shallow saddle point separating the looped and unlooped states. In panel (*B*), sub-pN tension gently extends DNA in the absence of imposed supercoiling, and the work associated with drawing the two operator sites together increases the energy barrier, effectively attenuating loop formation. These conditions correspond to a magnetic tweezer measurement in which the magnets exert tension but are not rotated to twist the DNA as shown in the superimposed cartoon. However, in plectonemic DNA as shown in the cartoon superimposed on panel (*C*), operator sites can juxtapose as DNA segments slither past each other in the plectoneme. This one-dimensional search for juxtaposition between looped and unlooped states changes the dynamics of looping with respect to the three-dimensional searches required in torsionally unrestrained DNA tethers.

Supercoiling induces ergodicity within a biologically relevant timescale

The TPM records in this work were between 20 and 30 minute-long, slightly below, or equal to the doubling time of *E. coli* which is approximately 30 minutes in the laboratory (Gibson et al., 2018). The heterogeneity of looping probabilities observed in these records without supercoiling were extreme and seemingly at odds with a molecular system designed to respond to the presence of lactose. Such a system was expected to be ergodic, such that sufficiently long observations of single members of the ensemble would have exhibited the statistical behavior of the whole ensemble. Several much longer, five-hour, recordings of LacI-mediated looping in torsionally relaxed DNA were then acquired using TPM (Supplemental Figure S9) and the looping probabilities were measured over temporal windows of different lengths, ranging from 10 min to the entire 5 hour-long recording. Figure 5A is an overlay of the cumulative probability distributions for looping percentages calculated for entire 5-hour records (black) or divided into shorter segments of 10 (blue), 30 (green), 40 (red), 60 (cyan), 80 (magenta), and 100 (yellow) min. Comparison of these distributions shows that recordings greater than or equal to 60 min (cyan) produce distributions like the five-hour (black) distribution in which all average looping probabilities fell between 0-30%. Observations for shorter periods exhibit a tail of high looping probabilities that is not present in distributions from longer observations. Thus, at least 60 min of observation are required to accurately sample the dynamics of LacI-mediated looping in a DNA construct containing the O1 and O2 operators separated by 400 bp; i.e. ergodicity is attained with recordings of no less than 60 min. This is due to the inherent stochastic nature of protein-mediated looping. If, however, DNA molecules are supercoiled, the reduced dimensionality modulating juxtaposition of the protein binding sites accelerates dynamics such that all DNA tethers exhibit similar looping probability and the statistical behavior of the ensemble can be revealed in much shorter observations of a single molecule. Indeed, analysis of looping probability in records for unwound DNA show that a cumulative distribution of looping probabilities equivalent to that attained in 20 min-long measurements is achieved in just 12 minutes (Figure 5B, Supplemental Figure S10). Thus, looping dynamics in supercoiled DNA are deterministic within the time scale of the doubling time of the bacteria, effectively the cell cycle.

Conclusion

Recently, LacI was observed to hop along the double helix (Marklund et al., 2020). This feature together with negative supercoiling is probably key for the protein to efficiently locate a binding site, contact a secondary binding site, and maintain a constant ratio of looped versus unlooped states in the various states of tension and torsion that likely develop during the cell cycle. This ratio gives a definitive regulatory outcome to looping based on inherently stochastic molecular activity. Additional parameters may contribute to achieving a specific outcome, but for straightforward protein-mediated looping, DNA supercoiling appears to be key.

Acknowledgments

We are grateful to Todd Lillian at the University of Southern Alabama for critical discussion. This work was supported by grants from the National Institutes of Health to L.F. (R01 GM084070) and F.L (1R21AI125973-01A1). Kathleen Matthews at Rice University generously provided the LacI protein. Plasmid pRLM118 was a gift from Roger McMacken (Johns Hopkins University).

Author Contributions

Conceptualization, D.D., L.F., Y.Y., S.K.; Methodology, S.K., Y.Y., W.X., D.D., F.L.; Software, S.K.; Formal Analysis, Y.Y., W.X., S.K., A.Z.; Investigation, S.K., Y.Y., A.Z., W.X.; Writing – Original Draft, L.F., Y.Y., W.X., A.Z.; Writing, Reviewing, Editing, L.F., D.D.; Funding Acquisition, L.F., F.L.; Resources, F.L.

Declaration of Interests

The authors declare that they have no competing interests.

Figures

Figure 1. The looping probabilities of different DNA tethers vary widely. (**A**) The calculated looping probabilities of individual tethers exposed to a range of LacI concentrations are summarized in a box-whisker plot. The whiskers span the entire range of probabilities of the ensemble of DNA tethers monitored in each condition. As the LacI concentration was titrated from 0 to 20 nM, the looping probability increased from 0 to approximately 45 and then fell again to 0 when repressor molecules saturated the binding sites. Note however, that at each concentration of LacI, the looping probabilities varied from 0 to 100. The upper and lower borders of the boxes indicate the upper and lower quartiles. The midline and cross of each box indicate the median and average of the distribution of looping probabilities. Schematic diagrams of prevalent DNA/LacI configurations are depicted below their corresponding LacI concentrations. (**B**) Representative temporal records of the TPM excursion parameter $< \boldsymbol{\rho^2} >$ with 0.5 nM [LacI] are ranked by looping probability from 0 (top) to 1 (bottom). Unlooped states are depicted in red, and looped states are shown in blue and green corresponding to loops in anti-parallel or parallel configurations respectively. The actual $< \boldsymbol{\rho^2} >$ values are encoded using the color scale at right.

Figure 2. HU did not reduce the variation of looping probabilities amongst different tethers. (**A**) The calculated looping probabilities of individual tethers, exposed to 2.5 nM and a range of HU protein concentrations, are summarized in a box-whisker plot. The whiskers span the entire

range of probabilities of the ensemble of DNA tethers monitored in each condition. As the HU concentration was titrated from 0 to 1056 nM, the average looping probability progressively increased from 25 to just above 80. Note however, that at each concentration of HU, the looping probabilities for individual DNA tethers varied from 0 to 100. The upper and lower borders of the boxes indicate the upper and lower quartiles. The midline and cross of each box indicate the median and average of the distribution of looping probabilities. (**B**) Representative temporal records of the TPM excursion parameter $< \boldsymbol{\rho^2} >$ with 2.5 nM [LacI] and 66 nM [HU] are ranked by looping probability from 0 (top) to 1 (bottom). Unlooped states are depicted in red, and looped states are shown in blue and green corresponding to loops in anti-parallel or parallel configurations respectively. The actual $< \boldsymbol{\rho^2} >$ values are encoded using the color scale at right.

Figure 3. Supercoiling dramatically reduces the variation of looping probabilities amongst DNA tethers. (**A**) The calculated looping probabilities of individual tethers, exposed to 1 nM LacI and negatively supercoiled to varying degrees, are summarized in a box-whisker plot. The whiskers span the entire range of probabilities of the ensemble of DNA tethers monitored in each condition. As the supercoiling was varied from 0 to almost -5% (σ), the average looping probability progressively increased from 0 to 100. Note that at each level of supercoiling, the looping probabilities for individual DNA tethers formed compact distributions. The upper and lower borders of the boxes indicate the upper and lower quartiles. The midline and cross of each box indicate the median and average of the distribution of looping probabilities. The whiskers and quartiles are only distinct for intermediate values of negative supercoiling. For low and high levels of negative supercoiling the whiskers collapse to the median value. (**B**) Representative temporal records of the instantaneous lengths of DNA tethers exposed to 1 nM [LacI] while stretched by 0.45 pN of tension and supercoiled to σ = -2.5% are shown. Unlooped states are depicted in red, and looped states are shown in blue and green corresponding to loops in anti-parallel or parallel configurations respectively. The actual tether length values are encoded using the color scale at right.

Figure 4. Energy landscapes for loop closure by LacI in different conditions of tension and torsion. The illustrations at the left show possible conformations of DNA tethers corresponding to different separations between the operators. *A*-*C* are three hypothetical energy landscapes for a DNA tether under different conditions of torsion and tension are represented. The energy values are qualitatively encoded using the color scale at right. The *y*-axis indicates the distance between the protein binding sites that constitute the junction and may vary between zero and 133 nm for a 400 bp DNA segment. DNA supercoiling varies along the *x*-axis. Superimposed on each panel are illustrations of likely DNA conformations under the different conditions of torsion and tension.

Figure 5. Minimum observation times for ergodicity. Cumulative distributions of the looping probability for (**A**) different periods of TPM observations (10, 30, 40, 60, 80, 100 min) and (**B**) different periods of MT observations (2, 5, 10, 12, 15, 18 min) are plotted along with the cumulative distribution for the entire set of observations (black curves). All records used in this analysis were for 0.25 pN tension and 1.5% supercoiling. Only when observations last at least 60 min (*A*) or 12 min (*B*) do the cumulative distributions of the looping probabilities for individual molecules resemble the distributions for the maximum length observations. With shorter

observation periods, the looping probabilities measured for individual molecules varies widely. For example, in the TPM data in *A*, looping probabilities measured for molecules observed for 10-minute intervals (blue) displayed a significant fraction of high probabilities that did not appear for the molecules observed for 60 min or more, up to 5 hours, (black)). In *B*, looping probabilities spanning the entire range result for 2- or 5-min periods of observation but narrow to the 40-80% range when observation times are 12 min or longer.

STAR Methods

Preparation of Proteins and DNA constructs

LacI was provided by Kathleen Matthews (Rice University). *E. coli* HU protein was overexpressed in *E. coli* strain BE257recA (*C600 leu, pro, lac, tonA, str, recA*) carrying plasmid pRLM118 where the hupA and hupB genes are under control of the lambda PL promoter. To express and purify *E. coli* HU protein, the *E. coli* strain BE257recA/pRLM118 was grown in 4 liters of terrific broth containing 50 μg/mL of ampicillin at 30 °C with vigorous aeration to OD595 reaching ~0.7, and then switched to 42 °C by adding 500 mL of 66 °C terrific broth per liter and grown for an additional 50 min at 42 °C. The cells were harvested by centrifugation at 6,000 rpm 4 °C for 15 min. The supernatant was discarded, and the cell pellet was resuspended in a cold cell lysis buffer (25 mM HEPES-KOH, pH 7.6, 1 M KCl, 1 mM DTT, 0.25 mg/mL lysozyme, and 1 mM PMSF). The cells in the cold buffer were incubated on ice for 1 hour, then frozen in liquid nitrogen, and stored in a -80 °C freezer. On the following day, the *E. coli* cells were thawed at a 4 °C water bath. After the thawing, the cell lysate was sonicated on ice six times at 30 W with 2 min interval between each sonication and centrifugated at 18,000 rpm for 60 min. The supernatant was dialyzed against buffer A (25 mM HEPES-KOH, pH 7.6, 50 mM NaCl, 1 mM DTT, 0.25 mg/mL lysozyme, 10% glycerol, and 1 mM PMSF) overnight and then loaded onto a 40 mL SP Sepharose FF column equilibrated with buffer A. The HU protein was eluted with a 300 mL NaCl gradient of 0.1-0.6 M NaCl in buffer A. The peak fractions were pooled, dialyzed against buffer A overnight, and loaded onto a DNA-cellulose column. The HU protein was eluted with a 300 mL NaCl gradient of 0.1-0.6 M NaCl in buffer A. The purity of *E. coli* HU protein was monitored using 20% SDS-PAGE and the concentration was determined using the Lorry assay (Biorad). The purified *E. coli* HU protein is free of nuclease contaminations as determined in the Leng laboratory.

DNA constructs (Supplemental Figure 1) were built similarly to others previously described (Yan et al., 2018b). All DNA fragments for TPM experiments were amplified by PCR using pO1O2 (Fulcrand et al., 2016) or pZV_21_400 (Vörös et al., 2017) plasmids, as a templates, digoxigenin- and biotin-labeled sense and anti-sense primers (Integrated DNA Technologies, Coralville, IA, or Invitrogen, Life Technologies, Grand Island, NY, USA) (Table S1), dNTPs (Fermentas-Thermo Fisher Scientific Inc., Pittsburgh, PA, USA) and Taq DNA Polymerase (New England BioLabs, Ipswich, MA, USA). The final 831bp-long DNA amplicons contained centrally located O1 and O2 operators separated by 400 bp (O1-400-O2 DNA; Supplemental Figure S1A).

DNA tethers used in the MTs measurements were built by amplifying a 3352, 2115 or 2011 bp-long main fragment containing the O1-400-O2 segment in the middle (Supplemental Figure S1B)

and using T7 ligase (New England Bio- Labs, Ipswich, MA, USA) to attach ~150 bp-long multiply digoxigenin-, or biotin-, labeled DNA fragments at opposite ends. These termini were necessary to securely attach one end of the main DNA fragment to an anti-digoxigenin-coated, flow-chamber surface and the other end to a streptavidin-coated bead.

The main fragments were amplified with a dNTP mix (Fermentas-Thermo Fisher Scientific Inc., Pittsburgh, PA, USA) and a forward primer containing an ApaI restriction site paired with a reverse primer containing an XmaI restriction site. A double digestion of the amplicon with ApaI and XmaI was purified prior to ligation. ~150 bp biotin- or digoxigenin-labeled DNA anchor fragments were generated by ApaI or XmaI restriction in the middle of 302 bp PCR amplicons produced using dATP, dCTP, dGTP, dTTP (Fermentas-Thermo Fisher Scientific Inc., Pittsburgh, PA, USA), and digoxigenin-11-dUTP (Roche Life Science, Indianapolis, IN, USA) or biotin-11-dUTP (Invitrogen, Life Technologies, Grand Island, NY, USA) in a molar ratio of 1:1:1:0.7:0.3. The product of ligation of the main fragment and two anchor fragments was purified and the total variation in DNA tether length, due to random placement of 30% biotin- or digoxigenin along the anchor fragments did not exceed 50 bp (16 nm) (Yan et al., 2018b) (Supplemental Figure S2).

Details about template and primers that were used to generate the TPM and MT DNA constructs are summarized in Supplemental Table 1.

Microchamber preparation

Parafilm gaskets were fashioned with a laser cutter (Universal Laser Systems, VLS 860, Middletown, CT) supported on microscope slides, and coverslips were placed on top. Each gasket included inlet and outlet reservoirs positioned just beyond the edges of the coverslip and connected through narrow inlet and outlet channels to the central observation area (Supplemental Figure S3). The assembly was heated briefly on a hot plate at the minimum setting to seal the components together. The narrow channels reduced evaporation of buffer while non-homogeneous flow through the triangular shape of the observation area produced a gradient of tether densities. DNA tethers in λ buffer (10 mM Tris-HCl (pH 7.4), 200 mM KCl, 5% DMSO, 0.1 mM EDTA, 0.1 mg/mL α-casein (Sigma-Aldrich, St. Louis, MO) were introduced into the chamber and attached through a single digoxigenin (TPM), or a multiply digoxigenin-labeled tail (MT) to the coverslip coated with anti-digoxigenin (Roche Life Science, Indianapolis, IN, USA). The opposite end of the DNA was attached to a streptavidin-coated bead via a single biotin (TPM), or a multiply biotin-labeled tail (MTs).

The beads used in TPM measurements were 0.32 μm diameter, streptavidin-coated polystyrene beads (Spherotech, Lake forest, IL, USA), while the beads used in MT measurements were 1.0 μm diameter, streptavidin-coated super-paramagnetic beads (Dynabead MyOne Streptavidin T1, Invitrogen, Grand Island, NY)

Tethered particle motion (TPM) experiments

All TPM experiments were conducted in λ buffer at room temperature. The LacI protein was introduced into the chamber before recording ~30 min or longer. For long experiments (up to 5 hours), the inlet and outlet of the chamber were sealed with grease after adding the LacI protein to avoid evaporation.

A Leica DM LB-100 microscope (Leica Microsystems, Wetzlar, Germany) with an oil-immersion objective (63X, NA 0.6–1.4) and differential interference contrast optics was used to observe tethered beads with a CV-A60 video camera (JAI, Copenhagen, Denmark). The absolute XY positions of each bead were recorded at 50 Hz with a custom Labview (National Instruments, Austin, TX, USA) program. Vibrational or mechanical drift in the position of each tethered bead was removed by subtracting the average position of multiple, stuck reference bead(s) within the same field of view (Han et al., 2009b; Kumar et al., 2014). The excursion of each tether was then calculated as $<\rho>_{8s}=<\sqrt{(x-<x>_{8s})^2+(y-<y>_{8s})^2}>_{8s}$, in which $<x>_{8s}$, and $<y>_{8s}$ are eight-second moving averages representing the coordinates of the anchor point of a bead. Changes in the excursion of the bead reflect conformational (length) changes of the DNA tether (Kovari et al., 2018; Priest et al., 2014b; Ucuncuoglu et al., 2017).

The beads that exhibited (*x*, *y*) position distributions with a ratio of the major to minor axes greater than 1.07, were discarded, since they were likely to be tethered by multiple DNA molecules (Kumar et al., 2014). The excursion data from the time records of the beads, in the same experimental conditions, which passed this "symmetry test" were pooled to generate probability distribution histograms. These summarized the average excursion distribution and, in the presence of LacI, they indicated three excursion peaks (two looped states and one unlooped state) (Yan et al., 2018b). The histogram of each selected temporal trace was fitted with three Gaussians, then the looping probability was calculated by dividing the area under the Gaussians corresponding to the two looped states (peaks with shorter excursion) by the total area under all three Gaussians. The mean value of looping probability under each protein condition were weighted by the length of each trace.

Magnetic tweezer experiments

The permanent magnets used in magnetic tweezer can move vertically along and rotate around the optical axis of the microscope to change the tension, or torsion, on the beads, and thus, twist the DNA tethers (Supplemental Figure 4 left panel). The hardware, as well as the bead tracking algorithms, have been previously described(Vörös et al., 2017). The *x*, *y*, *z*, and *t* coordinates of tethered beads and at least two stuck beads were recorded after calibration. Stretching DNA tethers under high tension (~2 pN) extends a 2115 or 2011 bp DNA template to ~0.7 or 0.67 μm, which was used to identify tethers with acceptable contour lengths. Twisting DNA tethers to measure the "hat curve" (Supplemental Figure S4 right panel) helps to identify and discard beads tethered by multiple DNA molecules. Selected tethers were recorded for 3 minutes under three different levels of tension (0.25, 0.45 or 0.75 pN) and at a series of twist settings to determine the DNA extension in each condition before adding LacI protein. After introducing 1 nM LacI protein, *x*, *y*, *z* and *t* data were recorded for 20 min at each selected tension and twist setting. The DNA extension *vs.* time data were then analyzed to identify probable looping events and calculate looping probability.

The position versus time records for each bead were taken holding the magnet at an integral number of turns. However, since there were multiple number of tethers in a field of view, the torsionally relaxed state of each DNA tether was not synchronized with the initial "zero" rotation of the magnet. Thus, the torsionally relaxed state of DNA molecule was obtained by fitting the extension versus twist curve for each molecule with a parabola (Supplemental Figure S5). Then

the effective number of turns applied to a DNA molecule was calculated by subtracting the center of hat curve from the turns introduced with the magnet. Then the supercoiling density was calculated as the effective number of turns divided by the twist of a torsionally relaxed DNA (number of base pairs/helical pitch).

Looping probability distributions as a function of observation periods

For individual tethers, the duration of looped (τ_l) and unlooped (τ_u) states was determined using the total variation denoising (TVD) algorithm (Little and Jones, 2010), and the looping probability was calculated as $P = \sum \tau_l / (\sum \tau_l + \sum \tau_u)$. When the time series was divided into shorter intervals, the looping probability was calculated as: $P_{l,T} = \sum_T \tau_l / (\sum_T \tau_l + \sum_T \tau_u)$, where $\sum_T$ refers to the sum within a time interval, *T*. Five-hour-long TPM measurements were sub-divided into intervals of 10, 20, 40, 60, 80, or 100 minutes. Twenty-minute-long magnetic tweezer records were sub-divided into intervals of 2, 5, 10, 12, 15, or 18 minutes. Distributions of $P_{l,T}$ and P were processed with the "ecdf" function of MatLab to obtain the empirical cumulative distribution of looping probabilities for each time interval.

Supplemental Information

Figure S1. Schematic diagrams of the DNA constructs used in TPM and MT measurements. Both constructs have the same central 400 bp loop region segment flanked by the O1 operator, toward the attachment to the glass surface of the microchamber (left, hatched) and O2 operator, toward the bead (right dashed arc). Lengths are given in base pairs.

Figure S2. The probability of labeling along the anchorage fragment as a function of the distance from the ligation junction with the main fragment. The anchorage fragments are prepared by digesting with XmaI or ApaI approximately 300 bp-long, biotin- or digoxigenin-labeled DNA amplicons centered on the multi-cloning site of pBluescriptKS+. Since the labels are attached to dUTP and the sequences are known, the probability of incorporating labeled nucleotides can be calculated as a function of the distance from the ligation junction (x) as the complement of the probability of not incorporating any label within that span. Since the fraction of labeled nucleotides was 0.3, the probability of labeling at each adenine nucleotide was 0.3. The probability that not even one label would have been incorporated within a segment x nucleotides long was $P_{unlabeled} = 0.7^{N_{A,x}}$, where $N_{A,x}$ is the number of adenines in the segment. Then the probability that at least one label will be incorporated in the segment is $P_{labeled} = 1 - 0.7^{N_{A,x}}$. There is about 0.95 probability that at least one label will be incorporated within 27 bp from the junction. The variation of the effective tether length due to labeling will range from 14 to 49 bp or about 12 nm.

Figure S3. An image of a triangular microchamber. A parafilm gasket cut with a laser cutter was placed between cleaned 24 X 50 mm and 22 X 22 mm coverslips and heated on a benchtop heater on a low setting for a few seconds to seal the assembly.

Figure S4. DNA supercoiling manipulation and looping by magnetic tweezers. DNA supercoiling refers to the over- or under-winding of a DNA molecule, which is often quantified as the ratio of the number of turns added, or subtracted, to a DNA molecule with respect to the number of helical turns in the torsionally relaxed state. (Left) Magnetic tweezers are a convenient tool with

which to modulate DNA supercoiling *in vitro*. A magnetic field within a microchamber attracts and orients a super para-magnetic bead attached to a single DNA molecule, applying tension to the DNA (dark, vertical arrow) and, upon rotation, twisting the DNA (light, circular arrow). For supercoiling, a DNA molecule must be anchored to the surface and the bead through multiple attachments. (Right) Twisting a 2115 bp DNA molecule under 0.3 pN of tension induces plectonemes that decrease the overall extension of the torsionally relaxed DNA (0 turns) as shown in this typical extension versus twist plot.

Figure S5. Finding the center of a twist versus extension curve. The number of turns added to a DNA molecule was calculated by fitting the extension versus twist curve with a parabola to determine the center.

Figure S6. Looping percentage before and after LacI replacement. Using tethered particle motion analysis, the percentage of time spent in the looped state was measured for a field of view of individual tethers in a first observation period. Then LacI was washed out and re-introduced. Following that the percentage of time spent in the looped state for the same set of tethers was assessed for a second observation period. Fitting the data with $y = x$ yields $R^2 = 0.530177$. This value of R^2 indicates that there was no correlation between the looping percentages measured for individual tethers in the two observation periods indicating that the percentage of looping is not conditioned by a given DNA molecule.

Figure S7. Low variation is observed for looping percentages measured in supercoiled DNA. A box-whisker plot summarizes the looping probabilities of DNA tethers in the presence of 1 nM LacI, under 0.25, 0.45 or 0.75 pN of tension and a range of negative supercoiling values (σ). The midline of the box indicates the median and the cross the mean of each distribution. The upper and lower borders of each box indicate the upper and lower quartiles of the measured looping probabilities. The whiskers reveal the complete range of the data. Supercoiling greatly restricted the ranges of data compared to corresponding data for DNA tethers that were not subject to mild tension and torsion as shown in Figures 1 and 2 of the main article.

Figure S8. HU binding significantly contracts but mildly unwinds DNA. A single 3352 bp DNA tether under 0.45 pN of tension in a magnetic tweezer was repeatedly wound and unwound in a buffer containing 200 mM KCl with various concentrations of HU ranging from 0 to 1000 nM. Increasing HU concentrations steadily reduced the extension of the DNA tether by nearly 30% but produced only very mild negative supercoiling. A parabolic curve (thick) was fit to each pair of winding and unwinding curves corresponding to different concentrations of HU. The vertex of the parabola represents the shift of the twist versus extension curve due to the supercoiling induced by HU protein binding to the DNA tether.

Figure S9. Long TPM recordings. Three representative recordings are shown from a set of fifty lasting over one hour. The blue dots represent the two-dimensionally projected amplitude of momentary excursions of the tethered bead; the red trace is the moving, 8-second time average of these values.

Figure S10. Sufficiently long observations are ergodic. (A) Distributions of the looping probabilities derived from TPM records lasting 5 hours (black) or split into shorter segments as

indicated (cyan). (B) Distributions of the looping probabilities derived from MT records lasting 20 min (blue) or split into shorter segments as indicated (brown). All data was recorded at 0.45 pN of tension and -1.5% supercoiling. The distributions of looping probabilities for the corresponding full-length record is included for comparison in each panel.

References

Bahloul, A., Boubrik, F., and Rouviere-Yaniv, J. (2001). Roles of Escherichia coli histone-like protein HU in DNA replication: HU-beta suppresses the thermosensitivity of dnaA46ts. Biochimie *83*, 219-229.

Benkovic, S.J., and Hammes-Schiffer, S. (2003). A perspective on enzyme catalysis. Science *301*, 1196-1202.

Berger, M., Gerganova, V., Berger, P., Rapiteanu, R., Lisicovas, V., and Dobrindt, U. (2016). Genes on a Wire: The Nucleoid-Associated Protein HU Insulates Transcription Units in Escherichia coli. Sci Rep *6*, 12.

Bido, A.T., Nordberg, B.G., Engevik, M.A., Lindquist, N.C., and Brolo, A.G. High-Speed Fluctuations in Surface-Enhanced Raman Scattering Intensities from Various Nanostructures. Applied Spectroscopy.

Brennan, L.D., Forties, R.A., Patel, S.S., and Wang, M.D. (2017). DNA Looping Mediates Nucleosome Transfer. Biophysical Journal *112*, 513A-513A.

Brutzer, H., Luzzietti, N., Klaue, D., and Seidel, R. (2010). Energetics at the DNA Supercoiling Transition. Biophysical Journal *98*, 1267-1276.

Cayley, S., Lewis, B.A., Guttman, H.J., and Record, M.T. (1991). Characterization of the cytoplasm of Escherichia coli K-12 as a function of external osmolarity: Implications for protein-DNA interactions in vivo. Journal of Molecular Biology *222*, 281-300.

Datta, S., and Seed, B. (2018). Influence of multiplicative stochastic variation on translational elongation rates. PLOS ONE *13*, e0191152.

Duderstadt, K.E., Geertsema, H.J., Stratmann, S.A., Punter, C.M., Kulczyk, A.W., Richardson, C.C., and van Oijen, A.M. (2016). Simultaneous Real-Time Imaging of Leading and Lagging Strand Synthesis Reveals the Coordination Dynamics of Single Replisomes. Molecular Cell *64*, 1035-1047.

Finzi, L., and Gelles, J. (1995). Measurement of lactose repressor-mediated loop formation and breakdown in single DNA molecules. Science *267*, 378-380.

Fulcrand, G., Dages, S., Zhi, X., Chapagain, P., Gerstman, B.S., Dunlap, D., and Leng, F. (2016). DNA supercoiling, a critical signal regulating the basal expression of the lac operon in Escherichia coli. Scientific reports *6*, 19243.

Gibson, B., Wilson, D.J., Feil, E., and Eyre-Walker, A. (2018). The distribution of bacterial doubling times in the wild. Proc Biol Sci *285*, 20180789.

Golding, I. (2018). Infection by bacteriophage lambda: an evolving paradigm for cellular individuality. Current Opinion in Microbiology *43*, 9-13.

Graham, J.E., Marians, K.J., and Kowalczykowski, S.C. (2017). Independent and Stochastic Action of DNA Polymerases in the Replisome. Cell *169*, 1201-+.

Guo, F., and Adhya, S. (2007). Spiral structure of Escherichia coli HUab provides foundation for DNA supercoiling. Proc Natl Acad Sci U S A *104*, 4309-4314.

Hammel, M., Amlanjyoti, D., Reyes, F.E., Chen, J.-H., Parpana, R., Tang, H.Y.H., Larabell, C.A., Tainer, J.A., and Adhya, S. (2016). HU multimerization shift controls nucleoid compaction. Science Advances *2*, e1600650.

Han, L., Garcia, H.G., Blumberg, S., Towles, K.B., Beausang, J.F., Nelson, P.C., and Phillips, R. (2009a). Concentration and length dependence of DNA looping in transcriptional regulation. PLoS ONE *4*, e5621.

Han, L., Lui, B.H., Blumberg, S., Beausang, J.F., Nelson, P.C., and Phillips, R. (2009b). Calibration of Tethered Particle Motion Experiements. In Mathematics of DNA Structure, Function and Interactions, C.J. Benham, S. Harvey, W.K. Olson, D.W.L. Sumners, and D. Swigon, eds. (New York: Springer), pp. 123-138.

Hnisz, D., Day, D.S., and Young, R.A. (2016). Insulated Neighborhoods: Structural and Functional Units of Mammalian Gene Control. Cell *167*, 1188-1200.

Kim, S.H., Ganji, M., Kim, E., van der Torre, J., Abbondanzieri, E., and Dekker, C. (2018). DNA sequence encodes the position of DNA supercoils. Elife *7*.

Koli, P., Sudan, S., Fitzgerald, D., Adhya, S., and Kar, S. (2011). Conversion of Commensal Escherichia coli K-12 to an Invasive Form via Expression of a Mutant Histone-Like Protein. mBio *2*.

Kovari, D.T., Yan, Y., Finzi, L., and Dunlap, D. (2018). Tethered Particle Motion: An Easy Technique for Probing DNA Topology and Interactions with Transcription Factors. In Single Molecule Analysis: Methods and Protocols, 2nd Edition, E.J.G. Peterman, ed., pp. 317-340.

Kumar, A., Chatterjee, S., Nandi, M., and Dua, A. (2016). Emergence of dynamic cooperativity in the stochastic kinetics of fluctuating enzymes. Journal of Chemical Physics *145*.

Kumar, S., Manzo, C., Zurla, C., Ucuncuoglu, S., Finzi, L., and Dunlap, D. (2014). Enhanced Tethered-Particle Motion Analysis Reveals Viscous Effects. Biophysical Journal *106*, 399-409.

Kundu, P., Saha, S., and Gangopadhyay, G. (2020). Stochastic Kinetic Approach to the Escape of DNA Hairpins from an alpha-Hemolysin Channel. Journal of Physical Chemistry B *124*, 6575-6584.

Lal, A., Dhar, A., Trostel, A., Kouzine, F., Seshasayee, A.S., and Adhya, S. (2016). Genome scale patterns of supercoiling in a bacterial chromosome. Nature Communications *7*, 11055.

Lipfert, J., Klijnhout, S., and Dekker, N.H. (2010). Torsional sensing of small-molecule binding using magnetic tweezers. Nucleic Acids Research *38*, 7122-7132.

Little, M.A., and Jones, N.S. (2010). Sparse Bayesian step-filtering for high-throughput analysis of molecular machine dynamics. In 2010 IEEE International Conference on Acoustics, Speech and Signal Processing (IEEE), pp. 4162-4165.

Lubelski, A., Sokolov, I.M., and Klafter, J. (2008). Nonergodicity mimics inhomogeneity in single particle tracking. Physical Review Letters *100*.

Macvanin, M., and Adhya, S. (2012). Architectural organization in E. coli nucleoid. Biochim Biophys Acta *1819*, 830-835.

Magdziarz, M., Weron, A., Burnecki, K., and Klafter, J. (2009). Fractional Brownian Motion Versus the Continuous-Time Random Walk: A Simple Test for Subdiffusive Dynamics. Physical Review Letters *103*.

Manzo, C., Zurla, C., Dunlap, D., and Finzi, L. (2011). Lambda genetic switch sensitivity depends on complex looping kinetics driven by nonspecific binding. European Biophysics Journal With Biophysics Letters *40*, 98-98.

Manzo, C., Zurla, C., Dunlap, D.D., and Finzi, L. (2012). The Effect of Nonspecific Binding of Lambda Repressor on DNA Looping Dynamics. Biophysical Journal *103*, 1753-1761.

Marklund, E., van Oosten, B., Mao, G., Amselem, E., Kipper, K., Sabantsev, A., Emmerich, A., Globisch, D., Zheng, X., Lehmann, L.C., *et al.* (2020). DNA surface exploration and operator bypassing during target search. Nature *583*, 858-861.

Meroz, Y., Sokolov, I.M., and Klafter, J. (2010). Subdiffusion of mixed origins: When ergodicity and nonergodicity coexist. Physical Review E *81*.

Milenkovic, S., Bodrenko, I.V., Lagostena, L., Gradogna, A., Serra, G., Bosin, A., Carpaneto, A., and Ceccarelli, M. (2020). The mechanism and energetics of a ligand-controlled hydrophobic gate in a mammalian two pore channel. Physical Chemistry Chemical Physics *22*, 15664-15674.

Miyashita, S., Ishibashi, K., Kishino, H., and Ishikawa, M. (2015). Viruses Roll the Dice: The Stochastic Behavior of Viral Genome Molecules Accelerates Viral Adaptation at the Cell and Tissue Levels. Plos Biology *13*.

Moore, C.C. (2015). Ergodic theorem, ergodic theory, and statistical mechanics. Proc. Natl. Acad. Sci. *112*, 1907-1911.

Morales, P., Rouviere-Yaniv, J., and Dreyfus, M. (2002). The histone-like protein HU does not obstruct movement of T7 RNA polymerase in Escherichia coli cells but stimulates its activity. Journal of Bacteriology *184*, 1565-1570.

Nelson, P.C. (2003). Biological Physics: Energy, Information, Life (New York: W. H. Freeman).

Neuman, K.C., Abbondanzieri, E.A., Landick, R., Gelles, J., and Block, S.M. (2003). Ubiquitous Transcriptional Pausing Is Independent of RNA Polymerase Backtracking. Cell *115*, 437-447.

Palmer, R.G. (1982). Broken ergodicity. Advances in Physics *31*, 669-735.

Phillips R., Kondev Y., Theriot J., and Garcia H. (2013). Physical Biology of the Cell (CRC Press).

Priest, D.G., Cui, L., Kumar, S., Dunlap, D.D., Dodd, I.B., and Shearwin, K.E. (2014a). Quantitation of the DNA tethering effect in long-range DNA looping in vivo and in vitro using the Lac and λ repressors. Proceedings of the National Academy of Sciences *111*, 349-354.

Priest, D.G., Kumar, S., Yan, Y., Dunlap, D.D., Dodd, I.B., and Shearwin, K.E. (2014b). Quantitation of interactions between two DNA loops demonstrates loop domain insulation in E. coli cells. Proceedings of the National Academy of Sciences of the United States of America *111*, E4449-E4457.

Qian, Z., Trostel, A., Lewis, D.E.A., Lee, S.J., He, X.M., Stringer, A.M., Wade, J.T., Schneiders, T.D., Durfee, T., and Adhya, S. (2016). Genome-Wide Transcriptional Regulation and Chromosome Structural Arrangement by GalR in E. coli. Frontiers in Molecular Biosciences *3*.

Record, M.T., Jr., Courtenay, E.S., Cayley, S., and Guttman, H.J. (1998). Biophysical compensation mechanisms buffering E. coli protein-nucleic acid interactions against changing environments. Trends Biochem Sci *23*, 190-194.

Rouvière-Yaniv, J., Yaniv, M., and Germond, J.-E. (1979). E. coli DNA binding protein HU forms nucleosome-like structure with circular double-stranded DNA. Cell *17*, 265-274.

Salerno, D., Brogioli, D., Cassina, V., Turchi, D., Beretta, G.L., Seruggia, D., Ziano, R., Zunino, F., and Mantegazza, F. (2010). Magnetic tweezers measurements of the nanomechanical properties of DNA in the presence of drugs. Nucleic Acids Research *38*, 7089–7099.

Szymanski, J., and Weiss, M. (2009). Elucidating the Origin of Anomalous Diffusion in Crowded Fluids. Physical Review Letters *103*.

Ucuncuoglu, S., Schneider, D.A., Weeks, E.R., Dunlap, D., and Finzi, L. (2017). Chapter Sixteen - Multiplexed, Tethered Particle Microscopy for Studies of DNA-Enzyme Dynamics. In Methods in Enzymology, M. Spies, and Y.R. Chemla, eds. (Academic Press), pp. 415-435.

van Loenhout, M.T.J., de Grunt, M.V., and Dekker, C. (2012). Dynamics of DNA Supercoils. Science *338*, 94-97.

Vlijm, R., Kim, S.H., De Zwart, P.L., Dalal, Y., and Dekker, C. (2017). The supercoiling state of DNA determines the handedness of both H3 and CENP-A nucleosomes. Nanoscale *9*, 1862-1870.

Vörös, Z., Yan, Y., Kovari, D.T., Finzi, L., and Dunlap, D. (2017). Proteins mediating DNA loops effectively block transcription. Protein Science *26*, 1427-1438.

Wang, M.D., Schnitzer, M.J., Yin, H., Landick, R., Gelles, J., and Block, S.M. (1998). Force and velocity measured for single molecules of RNA polymerase. Science *282*, 902-907.

Whitson, P.A., Hsieh, W.T., Wells, R.D., and Matthews, K.S. (1987). Influence Of Supercoiling And Sequence Context On Operator Dna-Binding With Lac Repressor. Journal of Biological Chemistry *262*, 14592-14599.

Xiao, B., Johnson, R.C., and Marko, J.F. (2010). Modulation of HU–DNA interactions by salt concentration and applied force. Nucleic Acids Research *38*, 6176-6185.

Yan, Y., Ding, Y., Leng, F.F., Dunlap, D., and Finzi, L. (2018a). Protein-mediated loops in supercoiled DNA create large topological domains. Nucleic Acids Research *46*, 4417-4424.

Yan, Y., Leng, F.F., Finzi, L., and Dunlap, D. (2018b). Protein-mediated looping of DNA under tension requires supercoiling. Nucleic Acids Research *46*, 2370-2379.

Zurla, C., Manzo, C, Dunlap, DD, Lewis, DEA, Adhya, S, Finzi, L (2009). Direct Demonstration and Quantification of Long-Range DNA looping by the Lambda Bacteriophage Repressor. Nucleic Acids Res *37*, 2789-2795.

Figure 1

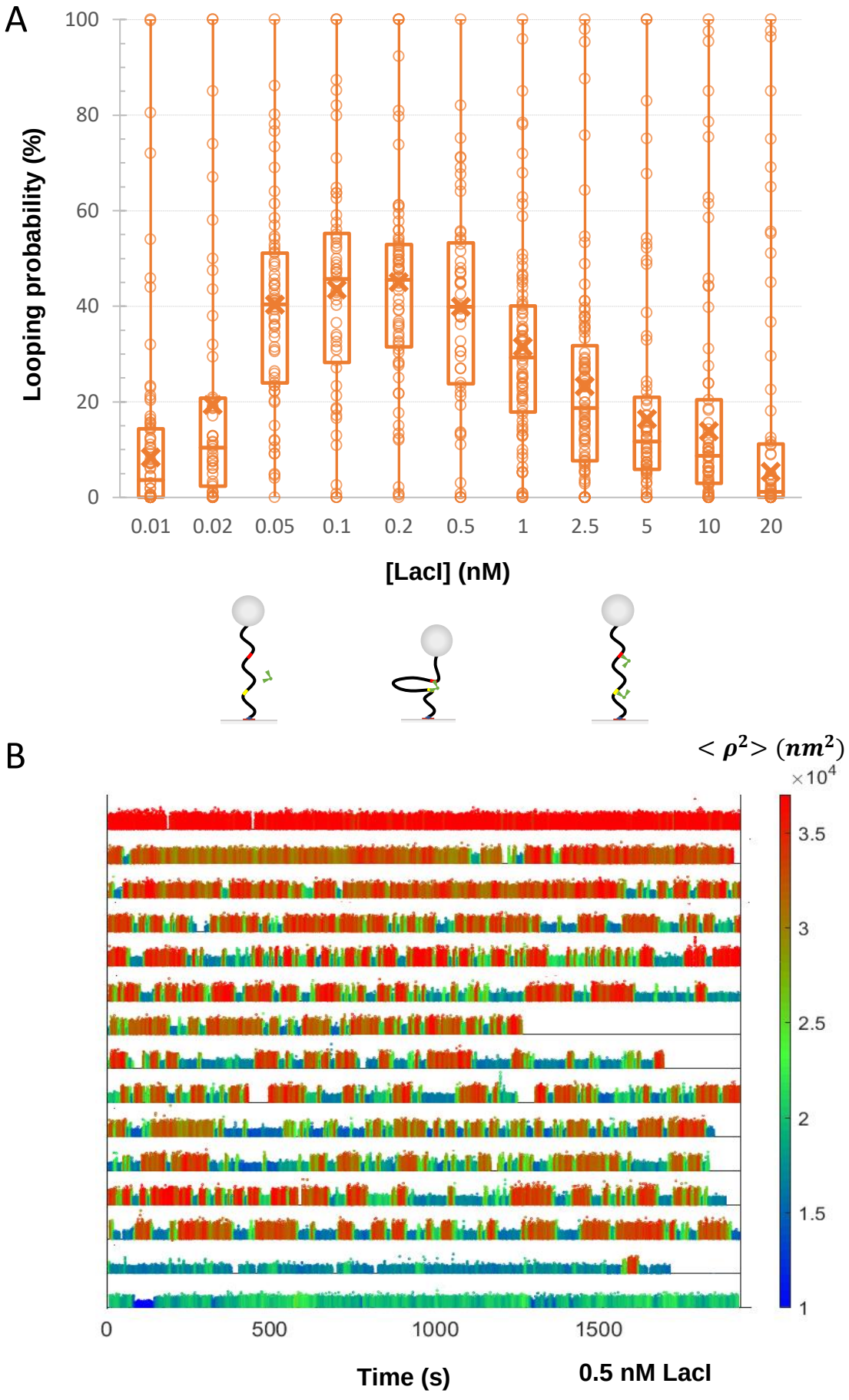

Figure 2

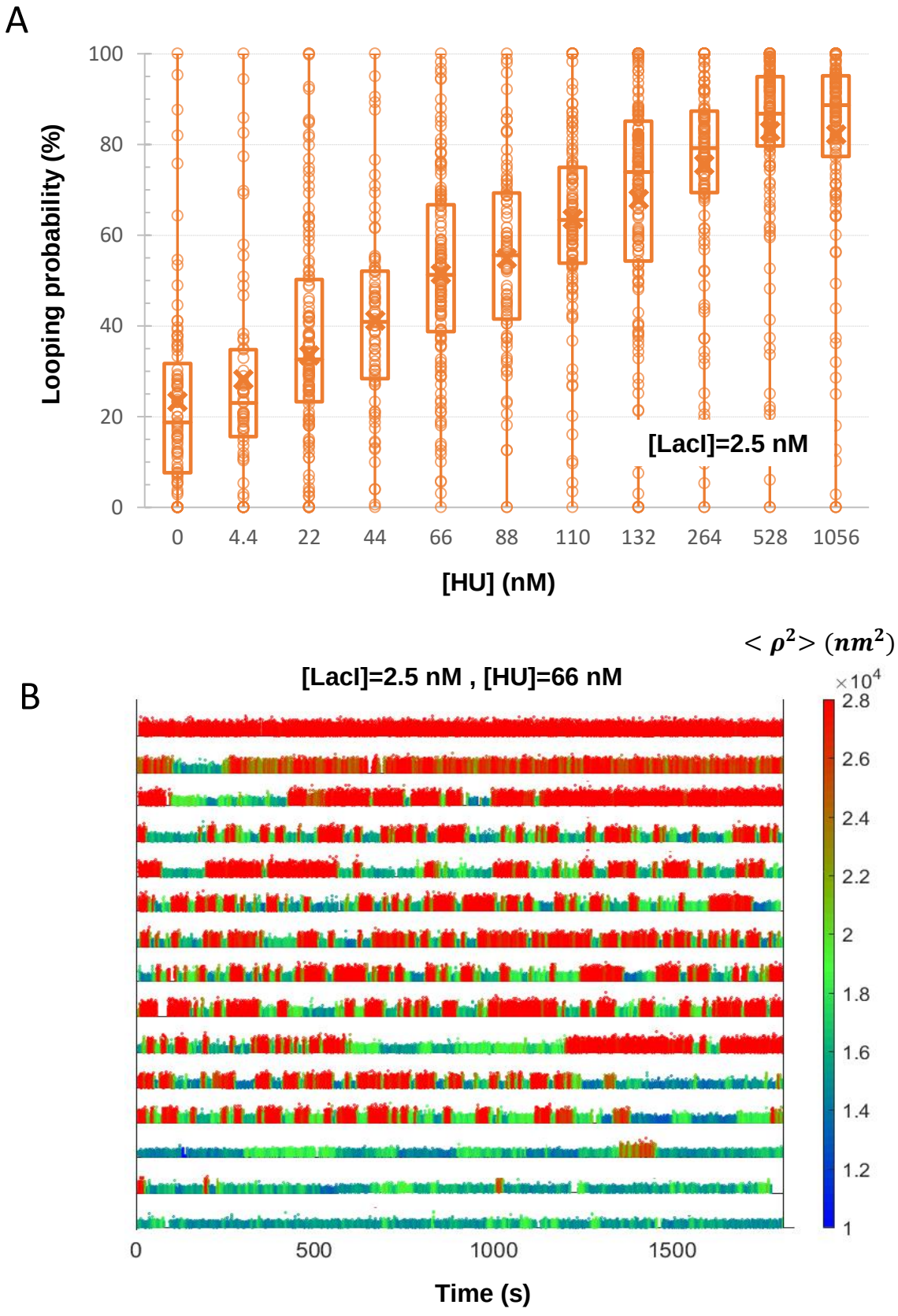

Figure 3

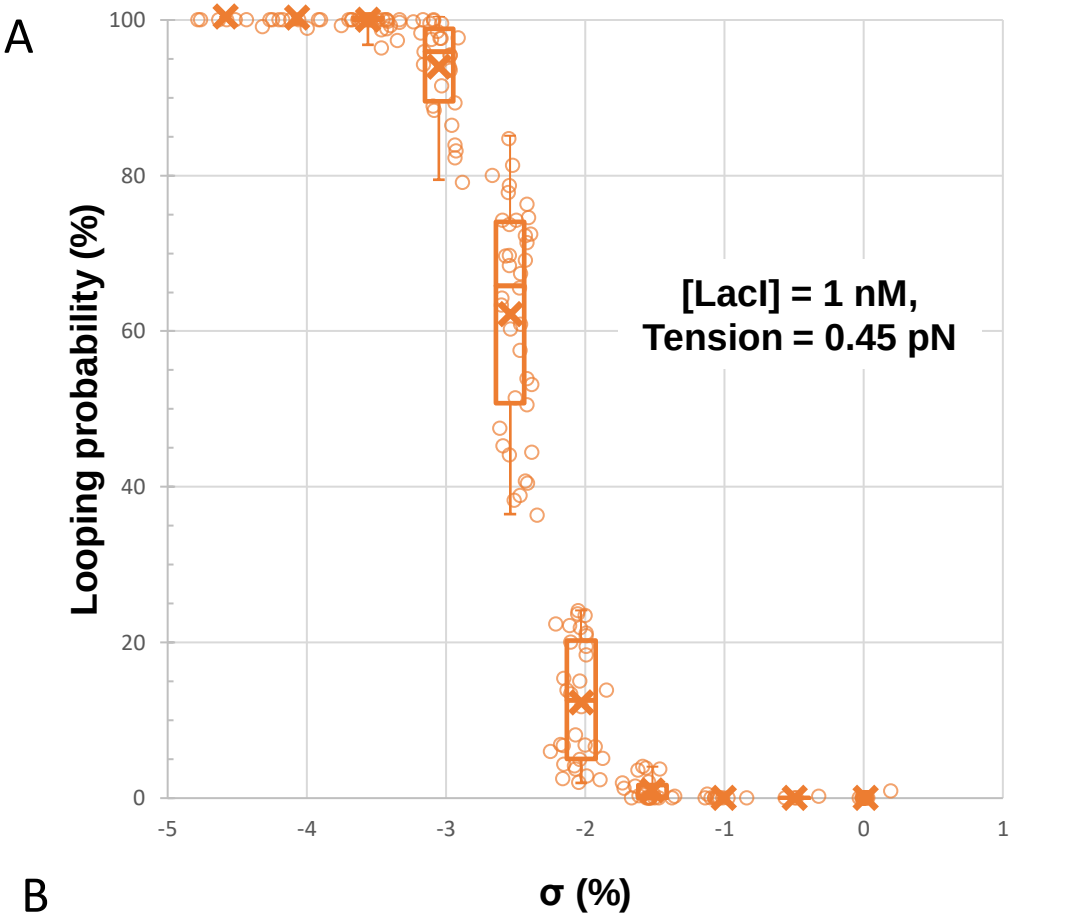

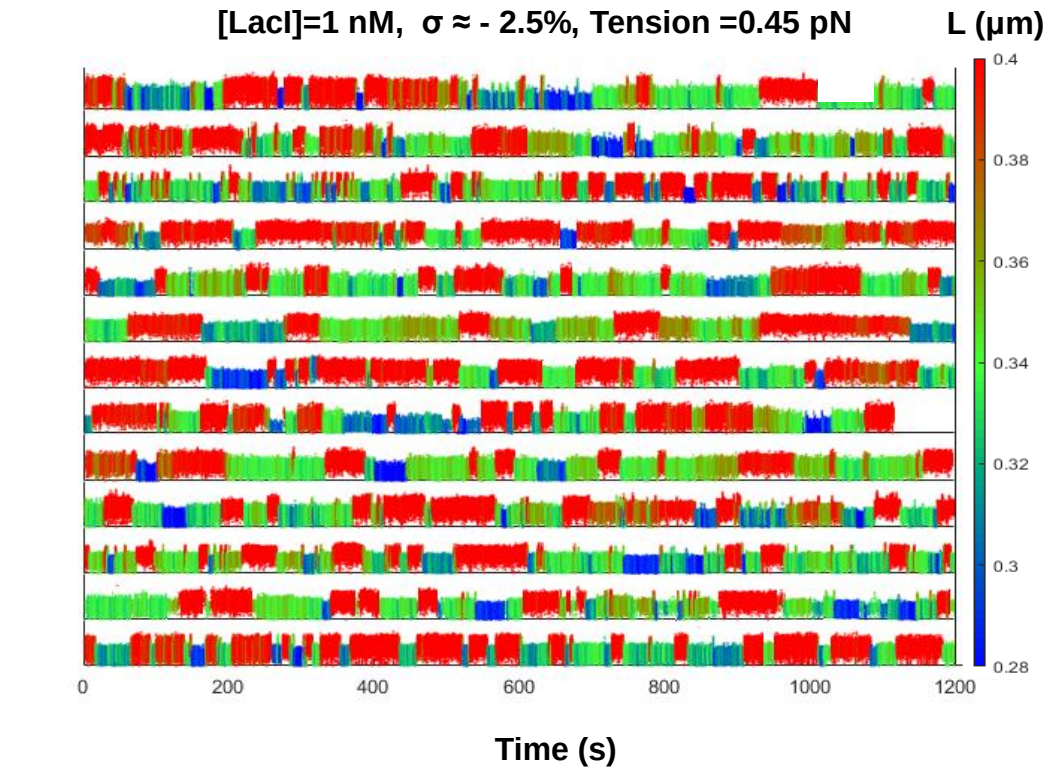

Figure 4

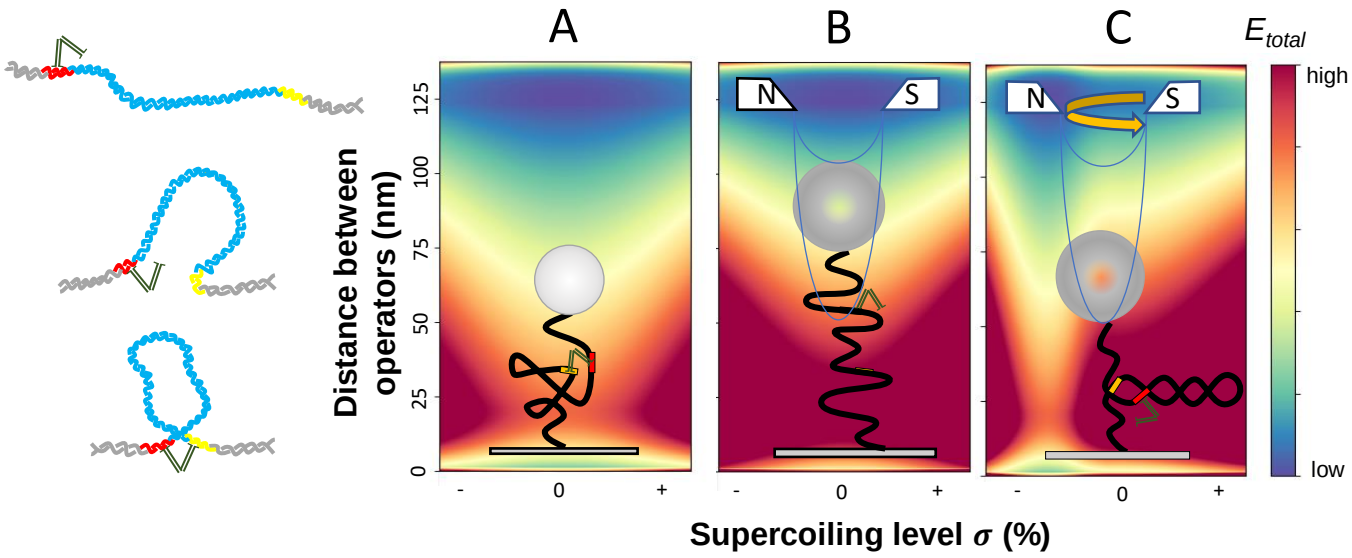

Figure 5